Toxicology in Vitro 91 (2023) 105628

Contents lists available at ScienceDirect

Toxicology in Vitro

journal homepage: www.elsevier.com/locate/toxinvit

Reactive oxygen species-dependent transient induction of genotoxicity by retene in human liver HepG2 cells

Caroline Scaramboni [a,e,*], Maria Lucia Arruda Moura Campos [a], Daniel Junqueira Dorta [a,c], Danielle Palma de Oliveira [b,c], Silvia Regina Batistuzzo de Medeiros [d], Marcos Felipe de Oliveira Galvão [e], Kristian Dreij [e,*]

[a] Department of Chemistry, Faculty of Philosophy, Sciences and Letters of Ribeirão Preto, University of São Paulo, Ribeirão Preto, SP 14040-903, Brazil
[b] School of Pharmaceutical Sciences of Ribeirão Preto, University of São Paulo, Ribeirão Preto, SP 14040-903, Brazil
[c] National Institute for Alternative Technologies of Detection, Toxicological Evaluation and Removal of Micropollutants and Radioactives (INCT-DATREM), Araraquara, SP, Brazil
[d] Department of Cell Biology and Genetics, Biosciences Center, Federal University of Rio Grande do Norte, Natal, RN, Brazil
[e] Institute of Environmental Medicine, Karolinska Institutet, Box 210, SE-171 77 Stockholm, Sweden

ARTICLE INFO

Keywords:
Biomass burning
Polycyclic aromatic hydrocarbons
Oxidative stress
ROS

ABSTRACT

Retene is a polycyclic aromatic hydrocarbon (PAH) emitted mainly by biomass combustion, and despite its ubiquity in atmospheric particulate matter (PM), studies concerning its potential hazard to human health are still incipient. In this study, the cytotoxicity and genotoxicity of retene were investigated in human HepG2 liver cells. Our data showed that retene had minimal effect on cell viability, but induced DNA strand breaks, micronuclei formation, and reactive oxygen species (ROS) formation in a dose- and time-dependent manner. Stronger effects were observed at earlier time points than at longer, indicating transient genotoxicity. Retene activated phosphorylation of Checkpoint kinase 1 (Chk1), an indicator of replication stress and chromosomal instability, which was in accordance with increased formation of micronuclei. A protective effect of the antioxidant *N*-acetylcysteine (NAC) towards ROS generation and DNA damage signaling was observed, suggesting oxidative stress as a key mechanism of the observed genotoxic effects of retene in HepG2 cells. Altogether our results suggest that retene may contribute to the harmful effects caused by biomass burning PM and represent a potential hazard to human health.

1. Introduction

Polycyclic aromatic hydrocarbons (PAHs) comprise a class of organic compounds released to the environment during incomplete combustion of organic material (Kim et al., 2013). Biomass burning, such as indoor firewood burning and wildfires, accounts for a high proportion of the global total atmospheric emissions of PAHs (Zhang et al., 2022). The presence of PAHs in the atmosphere is of great concern due to their mutagenic and carcinogenic potential (Turner et al., 2020).

Although hundreds of PAHs are currently known, most air quality and human biomonitoring studies focus on 16 priority compounds listed by the United States Environmental Protection Agency (U.S. EPA) in the 1970s (Keith, 2014). The list was based on the occurrence of PAHs in the environment, their toxicity, and on the availability of analytical standards and methods at the time, but its present relevance has been questioned by several authors (Andersson and Achten, 2015; Samburova et al., 2017; da Silva Junior et al., 2021a).

Retene (1-methyl-7-isopropylphenanthrene, Fig. 1) is an alkylated PAH that is not included in the list of 16 priority PAHs but has been used as a marker for biomass burning since the 1980s when it was reported as a thermal degradation product of abietic acid present in the resin of conifers (Ramdahl, 1983). Retene is the most abundant PAH found in atmospheric particulate matter (PM) collected at the Brazilian Amazon deforestation arc (de Oliveira Alves et al., 2011; de Oliveira Alves et al., 2014; de Oliveira Alves et al., 2015), at sugarcane-producing regions impacted by crop fires (Urban et al., 2016), and during wildfires in Portugal (Alves et al., 2011; Vicente et al., 2012, 2017). High levels of retene are also found during forest fire events (Yu et al., 2019). Additionally, retene has been used as a marker of residential wood-burning in urban areas, particularly during winter (Li et al., 2009; Křůmal et al.,

* Corresponding authors at: Institute of Environmental Medicine, Karolinska Institutet, Box 210, SE-171 77 Stockholm, Sweden.
E-mail addresses: carolinesc@usp.br (C. Scaramboni), kristian.dreij@ki.se (K. Dreij).

https://doi.org/10.1016/j.tiv.2023.105628
Received 7 March 2023; Received in revised form 24 May 2023; Accepted 8 June 2023
Available online 9 June 2023

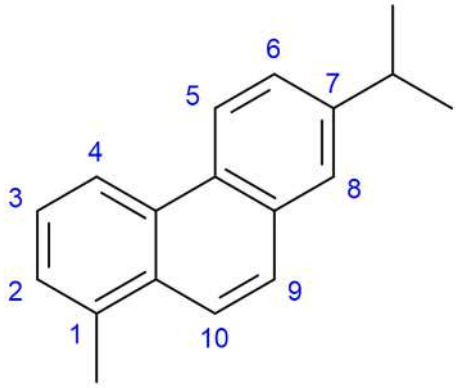

Fig. 1. Chemical structure of retene.

2017). Although biomass burning is the primary source of retene, coal combustion is a relevant source of this compound in indoor PM (Cui et al., 2022).

Besides being an atmospheric contaminant, retene has been associated with liquid effluents from pulp and paper mills, and sediments downstream of these industries, as it can be produced by anaerobic biotransformation of resin acids (Dahl et al., 2019). In this context, most studies related to the toxicity of retene are ecotoxicological assessments using aquatic organisms. Retene affects liver and heart functions of rainbow trout and zebrafish in early life stages (Scott et al., 2011; Rigaud et al., 2020; Wilsson et al., 2022) and induces genotoxicity in adult zebrafish, sea bass, and European eel (Gravato and Santos, 2002; Maria et al., 2005; da Silva Junior et al., 2021b). The cardiotoxicity of retene in fish has been linked to its strong antagonistic activity to the aryl hydrocarbon receptor (Scott et al., 2011). Although there are several studies on the aquatic ecotoxicity of retene, studies concerning its effects on humans are still incipient, despite its ubiquity in biomass burning PM.

In the context of new approach methodologies (NAMs) for toxicity testing, *in silico* and *in vitro* approaches stand out as alternatives to animal use. Currently, few studies have applied quantitative structure-activity relationship (QSAR) models to assess the genotoxicity, mutagenicity, and carcinogenicity of retene (Gbeddy et al., 2020), and more such studies are warranted (da Silva Junior et al., 2021a). Regarding *in vitro* testing, no mutagenic activity was detected in *Salmonella Typhimurium* strains TA98, TA97a, TA100, and TA102 (base-substitution, frameshift mutation, transition mutation, and transversion mutation strains), with and without metabolic activation (Møller et al., 1985; Peixoto et al., 2019). In mammalian systems, studies with human A549 lung cancer cells indicated that retene caused DNA damage, increased micronuclei frequency and promoted cell death and oxidative stress (de Oliveira Alves et al., 2017; Peixoto et al., 2019). In a study with human SK-N-SH neuroblastoma cells, retene mainly caused effects related to oxidative stress: increased levels of reactive oxygen species (ROS), decreased mitochondrial membrane potential, increased lipid peroxidation, and up-regulated oxidative stress-responsive genes (Sarma et al., 2017).

Since most PAHs exert their toxic effects after being metabolized to more reactive and electrophilic intermediates, it is of interest to assess the effects of retene using a more metabolic-competent cell line. Human hepatocarcinoma HepG2 cells express several phase I- and phase II-metabolizing enzymes and are capable of activating PAHs and other mutagens (Knasmüller et al., 1998) and suggested as a good model to study the toxicity of environmental chemicals (Jarvis et al., 2013). In addition, HepG2 cells are applied as a cell model for developing relative potency factors (RPF) to estimate the carcinogenic potential of single PAHs and complex environmental mixtures (Dreij et al., 2017; Kopp et al., 2018; de Oliveira Galvão et al., 2022). To the best of our knowledge, no previous studies have investigated the toxic effects of retene in HepG2 cells. Therefore, the aim of this study was to assess the *in vitro* cytotoxicity and genotoxicity of retene using HepG2 cells. To better understand the role of oxidative stress in the genotoxicity of retene in this type of cells, we also investigated intracellular levels of ROS and the protective effect of antioxidant towards ROS generation and DNA damage signaling.

2. Materials and methods

2.1. Chemicals and reagents

Retene (97%, CAS No. 483–65-8) was obtained from SPEX CertiPrep (Metuchen, NJ), and benzo[*a*]pyrene (B[*a*]P, ≥ 96%, CAS No. 50–32-8) from Sigma-Aldrich (Stockholm, Sweden). Sterile dimethyl sulfoxide (DMSO, >99.7%) was purchased from Merck KGaA (Darmstadt, Germany). Cell culture reagents were supplied by Gibco (Life Technologies, Stockholm, Sweden). Antibodies used for Western blotting were anti-phospho-Chk1 (Ser317; pChk1) and anti-phospho-H2AX (Ser139; γH2AX) from Cell Signaling Technology (Beverly, MA), and Cdk2 (M2) and secondary anti-rabbit antibodies from Santa Cruz (Santa Cruz, CA).

2.2. Cell culture and retene exposure

Human-derived hepatocellular carcinoma cells (HepG2) were obtained from American Type Culture Collection (ATCC, HB-8065, Rockville, MD). Cells were grown in Minimal Essential Medium (MEM) supplemented with 10% fetal bovine serum, 1 mmol/L sodium pyruvate, 0.1 mmol/L nonessential amino acids, 100 units/mL penicillin and 0.1 mg/mL streptomycin and maintained at 37 °C in 5% CO_2. The stock solution of retene was prepared by gentle evaporation of the original solvent with dry $N_2(g)$ until completely dry and then redissolved in DMSO. The retene concentration was determined by gas chromatography coupled with mass spectrometry (GCMS-QP2010, Shimadzu) or by spectrophotometry ($\varepsilon = 14996$ L/mol/cm, $\lambda = 300$ nm; Marzooghi, 2016) using a Cary 60 UV–Vis spectrophotometer (Agilent Technologies). The exposures used in this study ranged from 0.01 to 10 μmol/L and were selected considering the average concentration of retene in the PM collected at the sugarcane region (11 ng/m^3; Urban et al., 2016), the daily average volume of air breathed by an adult (16 m^3/day; US-EPA, 2011), an alveolar deposition rate of 20% (Heyder, 2004), and the volume of media used in the treatments (200 μL to 5 mL, depending on the assay). This range was also within the concentration range used in the previous studies with A549 cells (3.3 to 30 ng/mL, *i.e.*, 0.01 to 0.13 μmol/L) (de Oliveira Alves et al., 2017; Peixoto et al., 2019) and SK-N-SH cells (1.25 to 40 μmol/L) (Sarma et al., 2017). DMSO was also used to dissolve B[*a*]P and other positive controls, and it was used as negative control (NC) in all assays. The final DMSO concentration in the medium did not exceed 1.0% (*v*/v).

To determine whether the generation of ROS is an important mechanism of the genotoxic effect of retene, HepG2 cells were pre-treated with *N*-acetylcysteine (NAC, Sigma), which is a cell-permeable antioxidant involved in the induction of glutathione synthesis and scavenging of ROS (Shang et al., 2014). NAC was dissolved in phosphate-buffered saline (PBS) and filtered (0.2 μm) before use. Cells were treated with 2 mmol/L NAC for 1 h before exposure to retene.

2.3. MTT assay

The MTT assay measures metabolic activity of cells to reduce MTT (3-(4,5-dimethylthiazol-2-yl)-2,5-diphenyltetrazolium bromide) to a formazan salt and is widely used to assess cell viability (Mosmann, 1983). HepG2 cells (5×10^4/well) were plated in 96-well plates (Corning Inc., Corning, NY) and incubated for 24 h before exposure. Cells were exposed to retene for 24, 48 and 72 h. DMSO and carbonyl cyanide-3-chlorophenylhydrazone (CCCP, 10 μmol/L) were used as negative and positive controls, respectively. Following exposure, cells

were incubated with MTT solution (0.5 mg/mL) in Dulbecco's Modified Eagle Medium (DMEM) without phenol red for 3 h. The produced formazan salt was dissolved in DMSO, and plates were analyzed spectrophotometrically at 570 nm (SpectraMax i3x, Molecular Devices).

2.4. Comet assay

DNA strand breaks were detected using the alkaline comet assay according to the protocol described by Tice et al. (2000). HepG2 cells (1×10^6/well) were plated in 12-well plates (Corning Inc., Corning, NY) and incubated for 24 h before exposure. Cells were exposed to retene for 4 and 24 h. DMSO and methyl methanesulfonate (MMS, 0.13 μmol/L, for 3 h) were used as negative and positive controls, respectively. Nucleoids were visualized using a fluorescence microscope Olympus Bx50 (Olympus America INC), and tail intensity (DNA percentage in the comet tail) was measured using the Comet assay IV software (Perspectives, UK).

2.5. Cytokinesis-block micronucleus (CBMN) assay

The genomic instability biomarkers micronuclei (MN), nuclear buds (NB) and nucleoplasmatic bridges (NPB) were assessed by the CBMN assay, according to the guideline by OECD (2016). HepG2 cells (5×10^6) were seeded in 25 cm^2 flasks (Corning Inc., Corning, NY) and incubated for 24 h before exposure. Cells were exposed to retene for 20 h. DMSO and methyl methanesulfonate (MMS, 0.13 μmol/L) were used as negative and positive controls, respectively. After exposure, the treatment media was removed, cells were washed with PBS and incubated with fresh medium containing cytochalasin B (3 μg/mL, Sigma-Aldrich) for additional 28 h. Next, cold sodium citrate 1% solution was added to cell suspensions, which were posteriorly fixed with methanol:acetic acid solution (3:1, *v*/v) and added on pre-cleaned slides (Deckgläser, Germany). Cells were stained with a 5% Giemsa solution (Merck) for analysis using optical microscopy. Mononuclear and multi-nuclear cells were scored to calculate the Nuclear Division Index (NDI), and the numbers of MN, NB and NPB in 2000 binucleated cells were determined for each condition.

2.6. Micronucleus assay by flow cytometry

Micronuclei, hypodiploid nuclei, apoptotic and mid-to-late necrotic cells were assessed by flow cytometry, according to the method described by Vallabani et al. (2022). HepG2 cells (6×10^4/well) were seeded in 24-well plates (Corning Inc., Corning, NY) and incubated for 24 h before exposure. Cells were exposed to retene for 72 h, corresponding to 2–3 normal doubling periods of HepG2 cells (Le Bihanic et al., 2016). DMSO and etoposide (1.0 μmol/L) were used as negative and positive controls, respectively. Cells were acquired on a BD Accuri™ C6 (BD Biosciences, Franklin Lakes, NJ) flow cytometer. In total, 10,000 gated nuclei were acquired per sample and data analysis was performed using the BD Accuri™ C6 Software.

2.7. Western blotting

Levels of phosphorylated checkpoint kinase 1 (Chk1) and H2AX histone were determined using Western blotting as previously described (de Oliveira Galvão et al., 2022). HepG2 cells (3×10^5/well) were plated in 6-well plates (Corning Inc., Corning, NY) and incubated for 24 h before exposure. Cells were exposed to retene for 4, 12, 24 and 48 h. DMSO was used as the negative control and B[*a*]P (3 μmol/L) was used as positive control. Dose-response curves of Chk1 and H2AX phosphorylation were based on exposure with eight different concentrations of retene for 48 h using GraphPad Prism 8 (GraphPad Inc.).

2.8. ROS formation

Mitochondrial superoxide production was measured using the MitoSOX™ Red mitochondrial superoxide indicator (M36008, Thermo Fisher Scientific, Waltham, MA) as previously described by Barron Cuenca et al. (2022). HepG2 cells (1×10^4/well) were plated in 96-well plates (Corning Inc., Corning, NY) and incubated for 24 h before exposure. Cells were exposed to retene for 4, 12, 24, 48 and 72 h. DMSO and B[*a*]P (1.5 μmol/L) were used as negative and positive controls, respectively. Fluorescence intensity was measured using a Tecan Infinite F 200 microplate reader and normalized to protein concentrations by Bradford assay.

2.9. Statistical analysis

All data are presented as mean values ± standard error (SE) of at least three independent experiments. Differences between dose groups and negative control were tested for significance ($p < 0.05$) using one- or two-way analysis of variance (ANOVA) followed by Dunnett's multiple comparison test. Differences between positive and negative controls were tested for significance ($p < 0.05$) using unpaired *t*-test. Statistical analysis was performed using GraphPad Prism (GraphPad Inc.).

3. Results

3.1. Minimal reduction of cell viability

MTT assay was used to determine HepG2 viability following retene exposure. Cell viability decreased in a dose-dependent manner after 24 h of exposure, reaching a decrease of 24% at 10 μmol/L ($p < 0.0001$; Fig. 2A). After 48 h of exposure, a clear dose dependence was no longer observed (Fig. 2B), and after 72 h the viability did not change significantly at any concentration tested compared to the negative control (Fig. 2C). Although the reduction on cell viability was significant for some concentrations at 24 and 48 h, the viability range was within 76–99% for all experiments, which indicates that retene is non-cytotoxic to HepG2 at the concentrations tested.

3.2. Increase of DNA damage and chromosomal instability

The induction of DNA strand breaks by retene in HepG2 cells was evaluated using the comet assay. Concentration-dependent DNA damage was observed 4 h post-exposure, with a significant 2- to 3-fold increase at 0.5 and 1.0 μmol/L compared to the negative control ($p < 0.05$–0.001; Fig. 3A), respectively. However, the DNA damage was not persistent as tail intensity averages decreased and were not significantly different from the negative control at any concentrations tested after 24 h of exposure (Fig. 3A).

The impact of retene on the chromosomal integrity of HepG2 cells was assessed by two approaches: CBMN assay scored by microscopy and the flow cytometry-based MN assay. For the CBMN method, retene significantly increased the frequency of MN and NB at the highest concentration by 1.8- and 3.3-fold ($p < 0.05$–0.01) compared to the negative control, respectively (Fig. 3B). No effects on the frequency of NPB were observed.

In addition to the quantification of MN and hypodiploid (HD) nuclei frequency, the flow cytometry-based scoring allows for determination of apoptotic and mid-to-late necrotic cells. Exposure to retene did not increase the number of apoptotic and necrotic cells compared to the negative control (Fig. S1), corroborating the MTT assay results. A concentration-dependent increase in MN and HD was observed, however, this increase was not significant compared to the negative control, due to high variation of the data (Fig. S1).

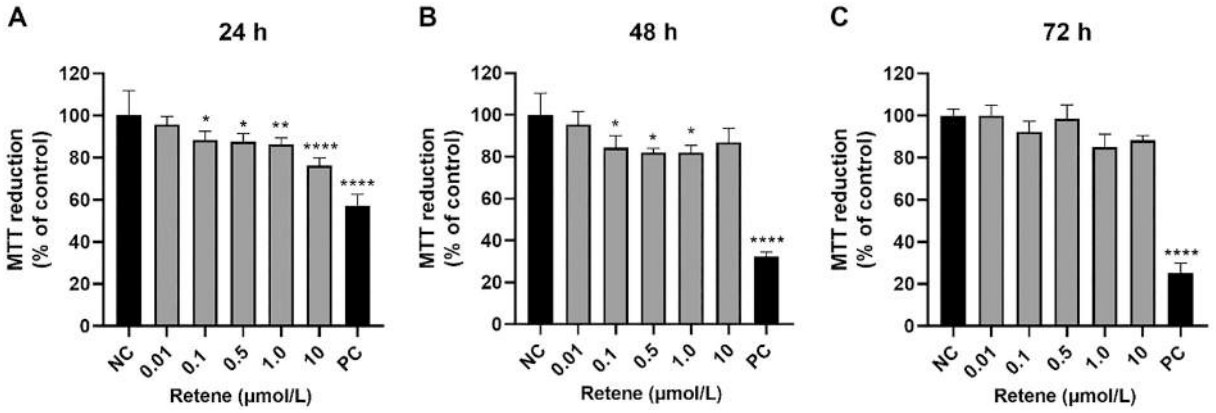

Fig. 2. Percentage of MTT reduction by HepG2 cells after exposure to retene at different concentrations for (A) 24, (B) 48 and (C) 72 h. CCCP (10 μmol/L) was used as a positive control (PC). Data represent mean ± SE ($n \geq 3$) with *p < 0.05, **p < 0.01 and ****p < 0.0001 as compared to the DMSO control (NC).

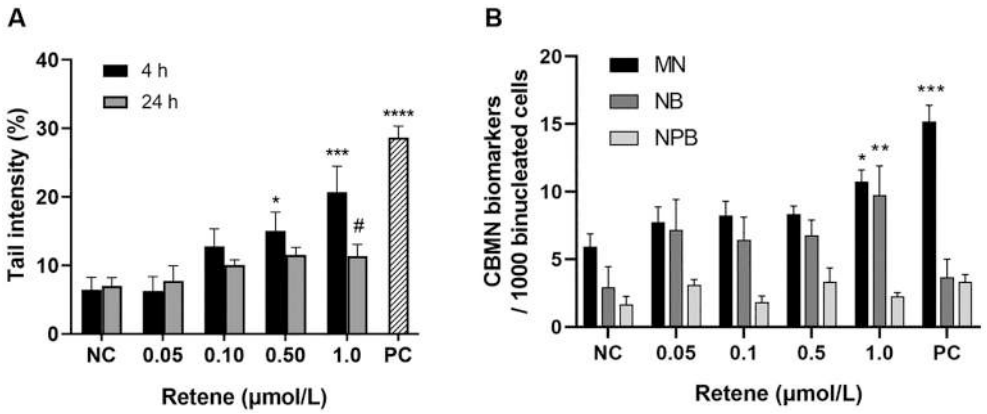

Fig. 3. (A) Tail intensity of HepG2 nucleoids after exposure to retene for 4 and 24 h assessed by comet assay. (B) Frequency of micronucleus (MN), nuclear buds (NB) and nucleoplasmatic bridges (NPB) in HepG2 cells exposed to retene for 48 h assessed by CBMN assay. MMS (0.13 μmol/L) was used as a positive control (PC). Data represent mean ± SE ($n = 3$). Columns with (*) were statistically different from the DMSO control (NC; *p < 0.05, **p < 0.01, ***p < 0.001, ****p < 0.0001). Colum with (#) was statistically different from the respective dose at 4 h (#p < 0.05).

3.3. No clear concentration-dependent activation of DNA damage signaling

The formation of DNA damage triggers the recruitment of signaling and DNA repair proteins. Cells were exposed to up to 10 μmol/L of retene for 48 h, and levels of phosphorylated Chk1 at Ser317 (pChk1) and H2AX at Ser139 (γH2AX) were determined by western blotting. Retene did not significantly induce pChk1 and γH2AX levels compared to negative control (Fig. 4). Comparing the results with previous data for the highly potent carcinogenic PAHs dibenzo[*a,l*]pyrene (DB[*a,l*]P) and B[*a*]P and the non-carcinogenic PAH phenanthrene from our lab using the same methodology, showed that the effect of retene was similar to phenanthrene and much less potent than DB[*a,l*]P and B[*a*]P (Dreij et al., 2017; de Oliveira Galvão et al., 2022). Because the effect of retene on pChk1 and γH2AX was below 2-fold, data were not appropriate for modeling, and it was not possible to calculate a relative potency factor (RPF) for retene.

3.4. Induction of DNA damage signaling in a time- and concentration-dependent manner

To further investigate the time-dependency of the DNA damage signaling induced by retene, we assessed the activation levels of pChk1 and γH2AX at time points earlier than 48 h. For all concentrations tested, pChk1 levels at 4 h were similar to the negative control (Fig. 5A). However, at 12 and 24 h after exposure pChk1 levels significantly increased 2.4-fold at the concentration of 10 μmol/L ($p < 0.001$–0.0001) and 1.8-fold in response to 1 μmol/L ($p < 0.01$). For all concentrations, a decrease in activation was observed at 48 h, suggesting that the DNA damage was repaired. γH2AX displayed a different time- and concentration-dependent pattern of activation (Fig. 5B). γH2AX levels increased above 2-fold in response to all concentrations of retene after 4 h of exposure ($p = 0.06$–0.13). At 12 h, all tested concentrations significantly induced γH2AX levels with a maximum of 2.9-fold in response to 1 μmol/L ($p < 0.05$–0.01). In contrast to pChk1, this was followed by a decline of γH2AX already at 24 h. Notably, the highest concentration of retene did not induce the strongest response of γH2AX at 12 h, but at 24 and 48 h, compared to the other concentrations. These results support the above-presented early and transient induction of DNA strand breaks (Fig. 3A) and the lack of a concentration-dependent DNA damage response at 48 h (Fig. 4).

3.5. Increase of mitochondrial superoxide production at short exposure

DNA damage can be induced as a result of an attack by reactive oxygen species (ROS) formed during the metabolism of chemicals. Therefore, we evaluated the generation of intracellular ROS by retene using the MitoSOX assay. The lowest concentration of retene (0.1 μmol/L) did not significantly induce ROS production at any of the time points studied (Fig. 6). For the higher concentrations, a clear time-dependency of ROS production was observed, with higher induction at early time intervals (4 and 12 h), reaching up to 1.9-fold at 12 h and 10 μmol/L ($p < 0.01$), then decreasing at later time intervals (Fig. 6).

3.6. ROS-dependent induction of DNA damage signaling

The induction of ROS production corroborated with the genotoxicity results, with early but transient induction of effects after exposure to

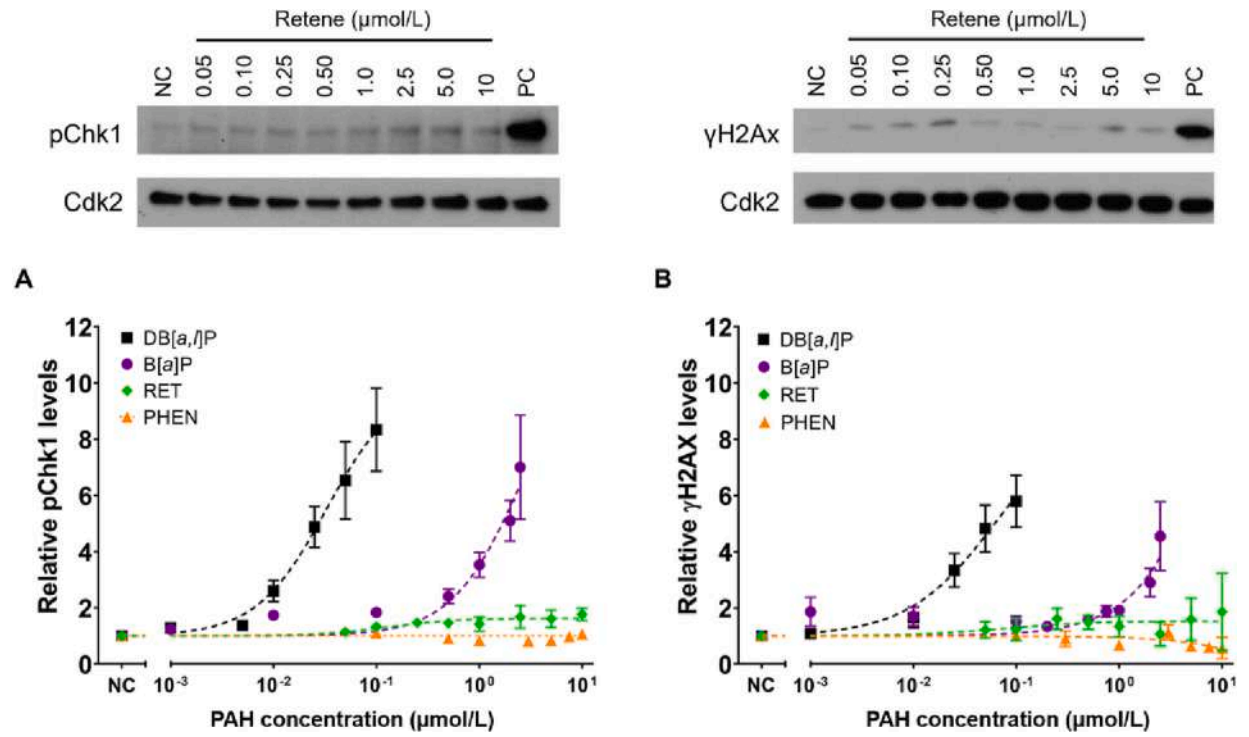

Fig. 4. Concentration-response curves based on levels of (A) pChk1 and (B) γH2AX in HepG2 cells exposed to retene (RET) for 48 h. Data represent mean ± SE ($n \geq 3$). Data for DB[*a*,*l*]P, B[*a*]P, and phenanthrene (PHEN) were obtained from Dreij et al. (2017) and de Oliveira Galvão et al. (2022). Representative blots are shown at the top. B[*a*]P 3 μmol/L was used as positive control (PC). NC = DMSO control. Cdk2 was used as loading control.

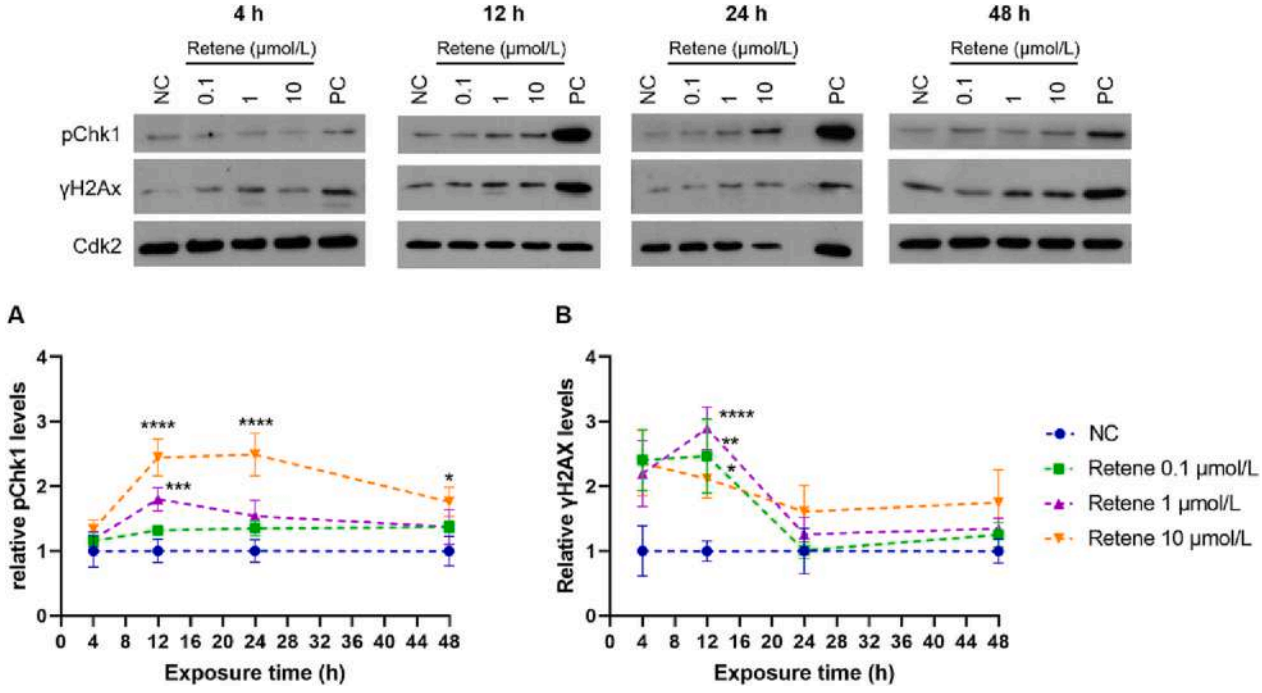

Fig. 5. Levels of (A) pChk1 and (B) γH2AX measured by western blot in HepG2 cells after different intervals of exposure to retene at different concentrations. Representative blots are shown at the top. B[*a*]P 3 μmol/L was used as a positive control (PC). Cdk2 was used as loading control. Data represent mean ± SE ($n \geq 3$) with $^{*}p < 0.05$, $^{**}p < 0.01$, $^{***}p < 0.001$, $^{****}p < 0.0001$ as compared to the DMSO control (NC).

retene. To further investigate if oxidative stress mediated the DNA damage caused by retene, we pretreated cells with NAC followed by exposure to retene and assessed the levels of ROS, pChk1 and γH2AX. Results showed that pretreatment of the cells with NAC reduced ROS levels close to the negative control levels at 4 and 12 h (Fig. S2). The time point chosen for western blotting was 12 h, as the highest ROS induction and DNA damage signaling levels were observed at this time interval.

Pre-treatment with NAC significantly reduced the levels of pChk1 of cells exposed to 1.0 and 10 μmol/L of retene ($p < 0.05$–0.0001) to

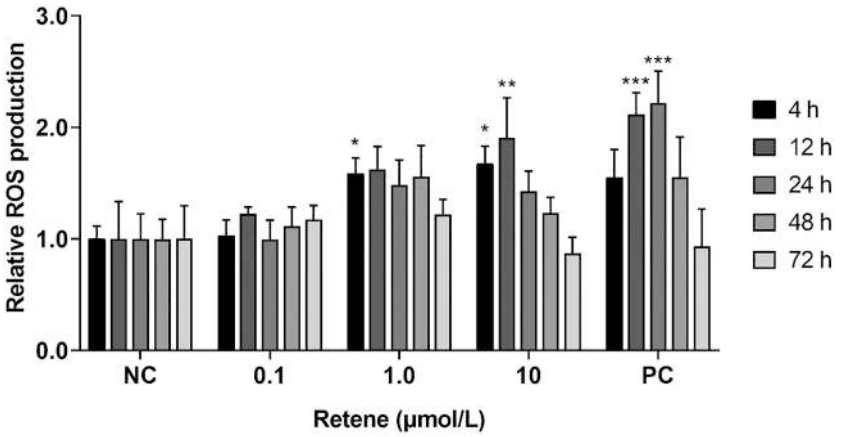

Fig. 6. Relative ROS production assessed by MitoSOX assay in HepG2 cells exposed to retene at different concentrations for 4, 12, 24, 48 and 72 h. B[*a*]P (1.5 µmol/L) was used as a positive control (PC). Data represent mean ± SE ($n \geq 3$) with $^{*}p < 0.05$, $^{**}p < 0.01$, $^{***}p < 0.001$, $^{****}p < 0.0001$ as compared to the DMSO control (NC).

negative control levels (Fig. 7A). Similarly, the levels of γH2AX were reduced to negative control levels in the presence of NAC, with a significant reduction at 1.0 µmol/L of retene ($p < 0.05$) (Fig. 7B). When the cells were exposed to B[*a*]P 3 µmol/L (positive control) in the presence of NAC, levels of pChk1 and γH2AX partially decreased by 32% and 46%, respectively. These results confirmed a ROS-dependent induction of DNA damage signaling in response to retene.

4. Discussion

Studying the toxicity of retene is of particular importance since this alkyl-PAH is present at high concentrations in PM emitted by biomass burning and, despite its abundance, few data have so far been reported regarding its potential hazard to human health. Here, we aimed at evaluating the toxicity of retene in HepG2 human liver cells, which have higher metabolic capacity than the cell lines previously used (de Oliveira Alves et al., 2017; Peixoto et al., 2019; Sarma et al., 2017). Our data showed that retene had minimal effect on cell viability, indicating that retene was non-cytotoxic to HepG2 cells at the concentrations tested. However, an early and transient effect was observed for the induction of genotoxicity, DNA damage signaling, and ROS formation, as summarized in Fig. 8.

These results differ from what was observed in studies using A549 lung cells, in which retene reduced cell viability only after 72 h of exposure, increased DNA strand breaks after 24 h of exposure and induced ROS production after 24 and 72 h of exposure (de Oliveira Alves et al., 2017; Peixoto et al., 2019). In these studies, the highest concentration used was 30 ng/mL, which corresponds to the concentration of

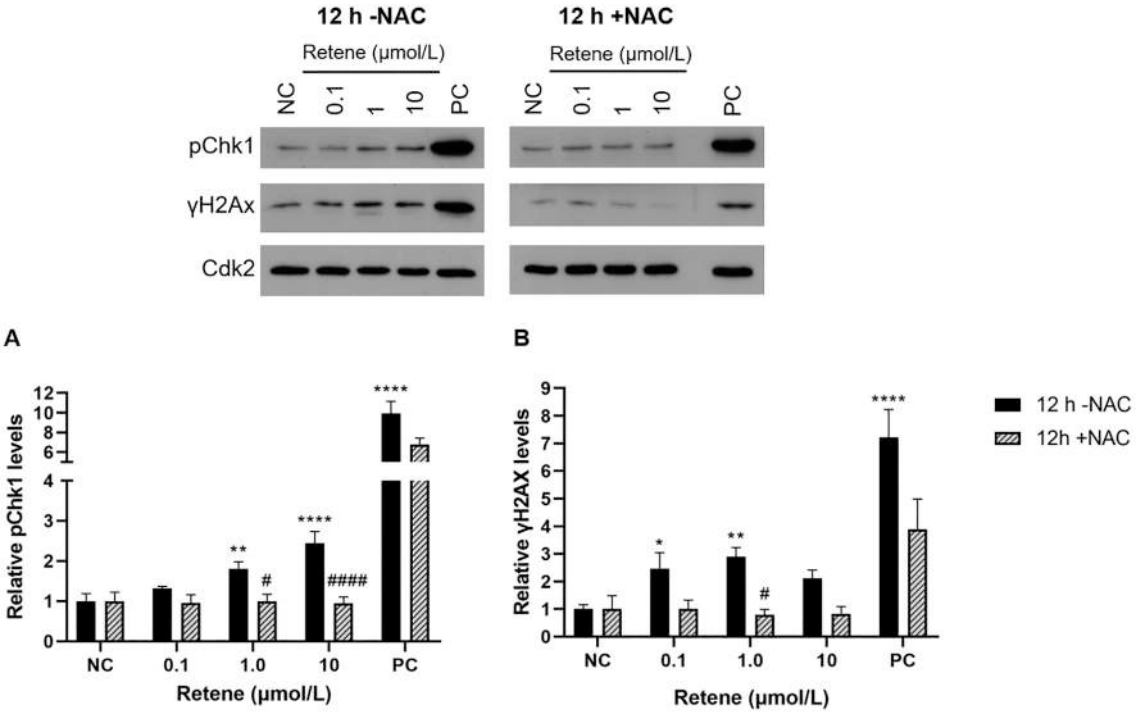

Fig. 7. Levels of (A) pChk1 and (B) γH2AX measured by western blot in HepG2 cells in response to retene alone (-NAC) or in combination with pretreatment of 2 mmol/L NAC (+NAC). Representative blots are shown at the top. B[*a*]P (3 µmol/L) was used as a positive control (PC). Cdk2 was used as loading control. Data represent mean ± SE ($n \geq 3$). Data with (*) were statistically different from DMSO control (NC; $^{*}p < 0.05$, $^{**}p < 0.01$, $^{***}p < 0.001$, $^{****}p < 0.0001$). Data with (#) were statistically different from the respective dose of retene alone (#$p < 0.05$, ####$p < 0.0001$).

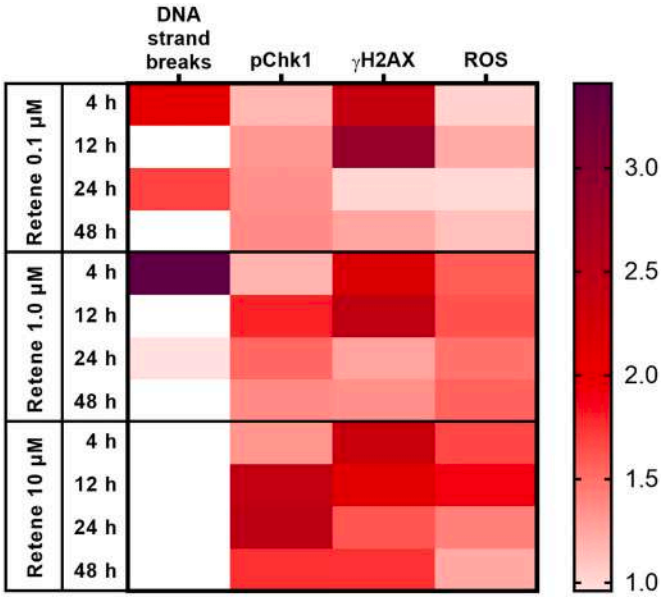

Fig. 8. Heatmap of genotoxicity, DNA damage signaling, and ROS formation in HepG2 cells exposed to three different concentrations of retene at different time points normalized to the negative control (fold-change). Dark red and purple colors indicate higher induction (above 2-fold) and light red colour indicates lower induction (below 2-fold). (For interpretation of the references to colour in this figure legend, the reader is referred to the web version of this article.)

0.1 µmol/L used in this work. Herein, most effects were more evident at higher concentrations *i.e.*, 1.0 and 10 µmol/L, suggesting that A549 cells are more sensitive to retene exposure than HepG2 cells. Additionally, for MN formation, concentrations of 0.05 and 0.1 µmol/L of retene increased MN frequency by 1.7- and 2.2-fold in A549 cells, respectively, while in HepG2 cells an increase of 1.8-fold was observed only for the concentration of 1.0 µmol/L.

The early effects observed in the hepatic cells when compared to lung cells may be due to the rapid retene metabolization by HepG2 cells (Huang et al., 2017). This may not be the case for A549 lung cells, which have a comparably lower metabolic capacity than HepG2 cells, exhibiting a limited cytochrome P450 (CYP) activity (Garcia-Canton et al., 2013). The major metabolic activation pathway of retene in HepG2 cells involves the formation of orthoquinones (Huang et al., 2017). The phase I and phase II enzymes involved in this pathway have not been fully identified yet, but it was hypothesized by Huang et al. (2017) that CYP1A1 and epoxide hydrolase are responsible for the formation of *trans*-dihydrodiols on the terminal rings of retene in HepG2 cells. *Trans*-Dihydrodiols can further be converted to catechols by aldoketo reductases (AKRs) such as AKR1C1, AKR1C2, and AKR1C3, also present in HepG2 cells. Catechols autoxidize into ortho-quinones triggering redox cycling and intracellular ROS formation (Shultz et al., 2011), which likely contributed to the oxidative stress-dependent genotoxicity observed here.

Evidence of metabolic activation on both terminal rings to form bis-orthoquinones has also been reported, although to a less extent than mono-orthoquinones (Huang et al., 2017). These bis-electrophiles have the potential to cross-link with DNA and protein, representing an additional potential mechanism for the genotoxicity of retene. Notably, A549 cells exhibit a lower level of induction of *CYP1A1* expression in response to PAHs compared to HepG2 cells (Genies et al., 2013). Therefore, a more efficient formation of retene *trans*-dihydrodiols is expected in the hepatic cells. However, A549 cells induce higher levels of AKRs, particularly AKRC1, than HepG2 cells in response to PAHs (Palackal et al., 2002; Genies et al., 2013), favoring the conversion of *trans*-dihydrodiols to ortho-quinones. Thus, CYP metabolism of retene in HepG2 cells may be faster, but the formation of quinones could be more efficient in A549 cells, explaining the higher sensitivity of this cell line to oxidative stress caused by retene. In addition, A549 cells were reported to be more sensitive than HepG2 cells to oxidative stress caused by other types of compounds, such as plant toxins and organophosphate flame retardants (An et al., 2016; Saxena et al., 2022). Moreover, HepG2 cells express higher levels of phase II enzymes than A549 cells in response to B[*a*]P, including glutathione transferase GSTP1 and UDP-glucuronosyltransferase UGT1A6 (Genies et al., 2013; Shi et al., 2016). This suggests that HepG2 phase II metabolism could detoxify the metabolites of retene more efficiently than A549 cells.

It was not possible to calculate a relative potency factor for retene using the *in vitro* model due to the low induction of the DNA damage signaling proteins at 48 h of exposure. A similar result was observed for retene's parent PAH phenanthrene (Dreij et al., 2017). The low potency of retene agrees with a recent study where the relative potency factor of was estimated to be 0.004 by a regression based QSAR model (Gbeddy et al., 2020), which is close to that of phenanthrene and pyrene (0.001) (Nisbet and LaGoy, 1992). When cells were exposed to retene for shorter time intervals, levels of phosphorylated DNA damage signaling proteins pChk1 and γH2AX increased up to 24 h of retene exposure followed by a decrease, indicating the process of activation and completion of DNA damage response and repair. The response of γH2AX was faster than pChk1, starting as early as 4 h, which was consistent with the comet assay and mitoSOX results. The phosphorylation of H2AX is an early event in cellular response to DNA double-strand breaks (DSB) (Fernandez-Capetillo et al., 2004). ROS formation induced by bioactivation of retene to ortho-quinones can cause DSB (Penning, 2017), triggering an early and acute response. This was also confirmed here by the observed reduction of γH2AX levels in the presence of the antioxidant NAC.

In contrast to γH2AX, pChk1 displayed a later response to retene, starting at 12 h and decreasing at 48 h to a level that was still significantly higher than the negative control, which indicated a more persistent level of activation. Chk1 is a downstream kinase that is predominantly activated through phosphorylation by the apical kinase ATR (ataxia telangiectasia and Rad3-related) in response to replication stress generated at stalled DNA replication forks (Gaillard et al., 2015). In addition to ROS-induced DNA lesions, PAH ortho-quinones can also covalently modify DNA resulting in bulky adducts (Penning, 2017) and B[*a*]P-7,8-dione induces stable dG and dA adducts in human lung cells (Huang et al., 2013). Since adducts derived from the major genotoxic metabolite B[*a*]P-7,8-dihydrodiol-9,10-epoxide induce replication stress (Fischer et al., 2018) and B[*a*]P exposure strongly induces levels of pChk1 (de Oliveira Galvão et al., 2022), it is likely that formation of stable adducts derived from retene quinone metabolites also may cause replication stress and induction of pChk1. In addition, the bis-orthoquinone metabolites of retene could form protein and DNA cross-links that would represent an impediment for replication forks. However, to the authors' knowledge it is not known to what extent and what type of covalent interactions occur between retene metabolites and DNA (Huang et al., 2017). A defective response to replication stress can lead to genome instability which can be observed as chromosome gain or loss (Gaillard et al., 2015), which is in accordance with the observed increase in micronuclei formation after retene exposure.

Contrasting mutagenicity results between *S. typhimurium* and mammalian models have been previously reported for PAHs and other organic compounds (Kirkland et al., 2007; Fowler et al., 2018; da Silva Junior et al., 2021a), which can be associated to differences in the types of mutations detected and in the metabolism of the models. The rat liver S9 mix generally used in the Ames test contains higher levels of CYP1A and 2B enzymes compared to other CYP forms, and phase II enzymes are mostly inactive in the S9 mix, as their cofactors are not added (Kirkland et al., 2007). Therefore, we suggest that metabolic activation of retene in HepG2 cells generates metabolites that cause ROS production and replication stress, processes that cause DNA damage and genome instability, indicating a potential hazard to human health.

5. Conclusion

This work provides new data on *in vitro* toxicity of retene. Based on our results on intracellular levels of ROS and the protective effect of antioxidant towards ROS generation and DNA damage signaling, we conclude that oxidative stress is an important mechanism of genotoxicity of retene in HepG2 cells. Another important mechanism can be replication stress, which together with ROS formation can lead to genetic instability, as observed *via* micronuclei formation. More studies on the toxicity of retene are important, since this PAH is consistently found at high concentrations in biomass burning particulate matter and may contribute to the harmful effects of this type of air pollution on human health.

Funding

This work was funded by the São Paulo State Research Foundation, Brazil (FAPESP, grant numbers #2018/16554–9 and INCT-DATREM 2014/50945–4), the National Council for Scientific and Technological Development, Brazil (MCT/CNPq Proc. Univ. 407699/2018–0, INCT-DATREM 465571/2014–0), the Swedish Cancer and Allergy Fund (grant number 10132) and the Swedish Research Council Formas (grant number 2019–). C.S. was supported by FAPESP (#2018/17931–0) and by a Joint Brazilian-Swedish Research Collaboration funded by the Swedish Foundation for International Cooperation in Research and Higher Education (STINT) and the Coordination for the Improvement of Higher Education Personnel (CAPES), Brazil (grant numbers BR2019–8515 and 88887.642068/2021–00).

Author contributions

Study conception: C.S., M.L.A.M.C., D.J.D. and K.D. Experimental planning and design: C.S., D.J.D., M.F.O.G. and K.D. Material preparation, data collection and analysis: C.S. Resources: D.J.D., D.P.O. and K.D. Funding acquisition: M.L.A.M.C., D.J.D., S.R.B.M., M.F.O.G. and K.D. Original manuscript: C.S. and K.D. All authors commented on previous versions of the manuscript. All authors read and approved the final manuscript.

Ethical approval

Not applicable.

Declaration of Competing Interest

The authors declare that they have no known competing financial interests or personal relationships that could have appeared to influence the work reported in this paper.

Data availability

Data will be made available on request.

Appendix A. Supplementary data

Supplementary data to this article can be found online at https://doi.org/10.1016/j.tiv.2023.105628.

References

Alves, C.A., Vicente, A., Monteiro, C., Gonçalves, C., Evtyugina, M., Pio, C., 2011. Emission of trace gases and organic components in smoke particles from a wildfire in a mixed-evergreen forest in Portugal. Sci. Total Environ. 409, 1466–1475. https://doi.org/10.1016/j.scitotenv.2010.12.025.

An, J., Hu, J., Shang, Y., Zhong, Y., Zhang, X., Yu, Z., 2016. The cytotoxicity of organophosphate flame retardants on HepG2, A549 and Caco-2 cells. J. Environ. Sci. Health A 51 (11), 980–988. https://doi.org/10.1080/10934529.2016.1191819.

Andersson, J.T., Achten, C., 2015. Time to say goodbye to the 16 EPA PAHs? Toward an up-to-date use of PACs for environmental purposes. Polycycl. Aromat. Compd. 35, 330–354. https://doi.org/10.1080/10406638.2014.991042.

Barron Cuenca, J., de Oliveira Galvão, M.F., Unlu Endirlik, B., Tirado, N., Dreij, K., 2022. In vitro cytotoxicity and genotoxicity of single and combined pesticides used by Bolivian farmers. Environ. Mol. Mutagen. 63 (1), 4–17. https://doi.org/10.1002/em.22468.

Cui, M., Chen, Y., Yan, C., Li, J., Zhang, G., 2022. Refined source apportionment of residential and industrial fuel combustion in the Beijing based on real-world source profiles. Sci. Total Environ. 826, 154101 https://doi.org/10.1016/j.scitotenv.2022.154101.

da Silva Junior, F.C., Felipe, M.B.M.C., de Castro, D.E.F., Araújo, S.C.S., Sisenando, H.C. N., de Medeiros, S.R.B., 2021a. A look beyond the priority: a systematic review of the genotoxic, mutagenic, and carcinogenic endpoints of non-priority PAHs. Environ. Pollut. 278, 116838 https://doi.org/10.1016/j.envpol.2021.116838.

da Silva Junior, F.C., Agues-Barbosa, T., Luchiari, A.C., de Medeiros, S.R.B., 2021b. Genotoxicity and behavioral alterations induced by retene in adult zebrafish. J. Environ. Chem. Eng. 9, 106518 https://doi.org/10.1016/j.jece.2021.106518.

Dahl, M., Survo, S., Valitalo, P., Kabiersch, G., Alitalo, O.S., Penttinen, O.P., Rantalainen, A.L., 2019. Identification of toxicants from a highly C10-C40 -contaminated sediment influenced by the wood industry: petroleum hydrocarbons or biogenic organic compounds? Environ. Toxicol. Chem. 38 (5), 936–946. https://doi.org/10.1002/etc.4380.

de Oliveira Alves, N., Vessoni, A.T., Quinet, A., Fortunato, R.S., Kajitani, G.S., Peixoto, M. S., de Souza, Hacon S., Artaxo, P., Saldiva, P., Menck, C.F.M., de Medeiros, S.R.B., 2017. Biomass burning in the Amazon region causes DNA damage and cell death in human lung cells. Sci. Rep. 7, 1–13. https://doi.org/10.1038/s41598-017-11024-3.

de Oliveira Galvão, M.F., Sadiktsis, I., Marques Pedro, T., Dreij, K., 2022. Determination of whole mixture-based potency factors for cancer risk assessment of complex environmental mixtures by in vitro testing of standard reference materials. Environ. Int. 166, 107345 https://doi.org/10.1016/j.envint.2022.107345.

de Oliveira Alves, N., Brito, J., Caumo, S., Arana, A., de Souza, Hacon S., Artaxo, P., Hillamo, R., Teinilä, K., de Medeiros, S.R.B., Vasconcellos, P.C., 2015. Biomass burning in the Amazon region: aerosol source apportionment and associated health risk assessment. Atmos Env. 120, 277–285. https://doi.org/10.1016/j.atmosenv.2015.08.059.

de Oliveira Alves, N., de Souza, Hacon S., de Oliveira Galvão, M.F., Peixoto, M.S., Artaxo, P., Vasconcellos, P.C., de Medeiros, S.R.B., 2014. Genetic damage of organic matter in the Brazilian Amazon: a comparative study between intense and moderate biomass burning. Environ. Res. 130, 51–58. https://doi.org/10.1016/j.envres.2013.12.011.

de Oliveira Alves, N., Matos Loureiro, A.L., dos Santos, F.C., Nascimento, K.H., Dallacort, R., Vasconcellos, P.C., de Souza, Hacon S., Artaxo, P., de Medeiros, S.R.B., 2011. Genotoxicity and composition of particulate matter from biomass burning in the eastern Brazilian Amazon region. Ecotoxicol. Environ. Saf. 74, 1427–1433. https://doi.org/10.1016/j.ecoenv.2011.04.007.

Dreij, K., Mattsson, Å., Jarvis, I.W.H., Lim, H., Hurkmans, J., Gustafsson, J., Bergvall, C., Westerholm, R., Johansson, C., Stenius, U., 2017. Cancer risk assessment of airborne PAHs based on in vitro mixture potency factors. Environ. Sci. Technol. 51, 8805–8814. https://doi.org/10.1021/acs.est.7b02963.

Fernandez-Capetillo, O., Lee, A., Nussenzweig, M., Nussenzweig, A., 2004. H2AX: the histone guardian of the genome. DNA Repair 3, 959–967. https://doi.org/10.1016/j.dnarep.2004.03.024.

Fischer, J.M.F., Zubel, T., Jander, K., Fix, J., Trussina, I.R.E.A., Gebhard, D., Bergemann, J., Bürkle, A., Mangerich, A., 2018. PARP1 protects from benzo[a] pyrene diol epoxide-induced replication stress and mutagenicity. Arch. Toxicol. 92, 1323–1340. https://doi.org/10.1007/s00204-017-2115-6.

Fowler, P., Meurer, K., Honarvar, N., Kirkland, D., 2018. A review of the genotoxic potential of 1,4-naphthoquinone. Mutat. Res. Genet. Toxicol. Environ. Mutagen. 834, 6–17. https://doi.org/10.1016/j.mrgentox.2018.07.004.

Gaillard, H., García-Muse, T., Aguilera, A., 2015. Replication stress and cancer. Nat. Rev. Cancer 15, 276–289. https://doi.org/10.1038/nrc3916.

Garcia-Canton, C., Minet, E., Anadon, A., Meredith, C., 2013. Metabolic characterization of cell systems used in in vitro toxicology testing: lung cell system BEAS-2B as a working example. Toxicol. in Vitro 27 (6), 1719–1727. https://doi.org/10.1016/j.tiv.2013.05.001.

Gbeddy, G., Egodwatta, P., Goonetilleke, A., Ayoko, G., Chen, L., 2020. Application of quantitative structure-activity relationship (QSAR) model in comprehensive human health risk assessment of PAHs, and alkyl-, nitro-, carbonyl-, and hydroxyl-PAHs laden in urban road dust. J. Hazard. Mater. 383, 121154 https://doi.org/10.1016/j.jhazmat.2019.121154.

Genies, C., Maitre, A., Lefebvre, E., Jullien, A., Chopard-Lallier, M., Douki, T., 2013. The extreme variety of genotoxic response to benzo[a]pyrene in three different human cell lines from three different organs. PLoS One 8 (11), e78356. https://doi.org/10.1371/journal.pone.0078356.

Gravato, C., Santos, M.A., 2002. Juvenile Sea bass liver biotransformation and erythrocytic genotoxic responses to pulp mill contaminants. Ecotoxicol. Environ. Saf. 53 (1), 104–112. https://doi.org/10.1006/eesa.2002.2196.

Heyder, J., 2004. Deposition of inhaled particles in the human respiratory tract and consequences for regional targeting in respiratory drug delivery. Proc. Am. Thorac. Soc. 1, 315–320. https://doi.org/10.1513/pats.200409-046TA.

Huang, M., Blair, I.A., Penning, T.M., 2013. Identification of stable benzo[a]pyrene-7,8-dione-DNA adducts in human lung cells. Chem. Res. Toxicol. 26, 685–692. https://doi.org/10.1021/tx300476m.

Huang, M., Mesaros, C., Hackfeld, L.C., Hodge, R.P., Zang, T., Blair, I.A., Penning, T.M., 2017. Potential metabolic activation of a representative C4-alkylated polycyclic

aromatic hydrocarbon Retene (1-Methyl-7-isopropyl-phenanthrene) associated with the Deepwater horizon oil spill in human hepatoma (HepG2) cells. Chem. Res. Toxicol. 30, 1093–1101. https://doi.org/10.1021/acs.chemrestox.6b00457.

Jarvis, I.W.H., Bergvall, C., Bottai, M., Westerholm, R., Stenius, U., Dreij, K., 2013. Persistent activation of DNA damage signaling in response to complex mixtures of PAHs in air particulate matter. Toxicol. Appl. Pharmacol. 266, 408–418. https://doi.org/10.1016/j.taap.2012.11.026.

Keith, L.H., 2014. The source of U.S. EPA's sixteen PAH priority pollutants. Polycycl. Aromat. Compd. 35 (2–4), 147–160. https://doi.org/10.1080/10406638.2014.892886.

Kim, K.H., Jahan, S.A., Kabir, E., Brown, R.J.C., 2013. A review of airborne polycyclic aromatic hydrocarbons (PAHs) and their human health effects. Environ. Int. 60, 71–80. https://doi.org/10.1016/j.envint.2013.07.019.

Kirkland, D., Pfuhler, S., Tweats, D., Aardema, M., Corvi, R., Darroudi, F., Elhajouji, A., Glatt, H., Hastwell, P., Hayashi, M., Kasper, P., Kirchner, S., Lynch, A., Marzin, D., Maurici, D., Meunier, J.R., Müller, L., Nohynek, G., Parry, J., Parry, E., Thybaud, V., Tice, R., Benthem, J., Vanparys, P., White, P., 2007. How to reduce false positive results when undertaking in vitro genotoxicity testing and thus avoid unnecessary follow-up animal tests: report of an ECVAM workshop. Mutat. Res. Genet. Toxicol. Environ. Mutagen. 628 (1), 31–55. https://doi.org/10.1016/j.mrgentox.2006.11.008.

Knasmüller, S., Parzefall, W., Sanyal, R., Ecker, S., Schwab, C., Uhl, M., Mersch-Sundermann, V., Williamson, G., Hietsch, G., Langer, T., Darroudi, F., Natarajan, A. T., 1998. Use of metabolically competent human hepatoma cells for the detection of mutagens and antimutagens. Mutat Res - Fundam Mol Mech Mutagen 402, 185–202. https://doi.org/10.1016/S0027-5107(97)00297-2.

Kopp, B., Dario, M., Zalko, D., Audebert, M., 2018. Assessment of a panel of cellular biomarkers and the kinetics of their induction in comparing genotoxic modes of action in HepG2 cells. Environ. Mol. Mutagen. 59 (6), 516–528. https://doi.org/10.1002/em.22197.

Křůmal, K., Mikuška, P., Večeřa, Z., 2017. Characterization of organic compounds in winter PM1 aerosols in a small industrial town. Atmos Pollut Res. 8, 930–939. https://doi.org/10.1016/j.apr.2017.03.003.

Le Bihanic, F., Di Bucchianico, S., Karlsson, H.L., Dreij, K., 2016. In vivo micronucleus screening in zebrafish by flow cytometry. Mutagenesis 31, 643–653. https://doi.org/10.1093/mutage/gew032.

Li, Z., Porter, E.N., Sjödin, A., Needham, L.L., Lee, S., Russell, A.G., Mulholland, J.A., 2009. Characterization of PM2.5-bound polycyclic aromatic hydrocarbons in Atlanta - seasonal variations at urban, suburban, and rural ambient air monitoring sites. Atmos Env. 43, 4187–4193. https://doi.org/10.1016/j.atmosenv.2009.05.031.

Maria, V.L., Correia, A.C., Santos, M.A., 2005. Anguilla anguilla L. liver EROD induction and genotoxic responses after retene exposure. Ecotoxicol. Environ. Saf. 61 (2), 230–238. https://doi.org/10.1016/j.ecoenv.2004.10.011.

Marzooghi, S., 2016. Phototoxic Target Lipid Model for Predicting the Toxicity of Polycyclic Aromatic Hydrocarbons and Petroleum to Aquatic Life. University of Delaware. https://udspace.udel.edu/handle/19716/21150 (Accessed 07 Dec 2022).

Møller, M., Hagen, I., Ramdahl, T., 1985. Mutagenicity of polycyclic aromatic compounds (PAC) identified in source emissions and ambient air. Mutat Res Genet Toxicol. 157, 149–156. https://doi.org/10.1016/0165-1218(85)90110-7.

Mosmann, T., 1983. Rapid colorimetric assay for cellular growth and survival: application to proliferation and cytotoxicity assays. J. Immunol. Methods 65, 55–63. https://doi.org/10.1016/0022-1759(83)90303-4.

Nisbet, I.C., LaGoy, P.K., 1992. Toxic equivalency factors (TEFs) for polycyclic aromatic hydrocarbons (PAHs). Regul. Toxicol. Pharmacol. 16 (3), 290–300. https://doi.org/10.1016/0273-2300(92)90009-X.

OECD - Organisation for Economic Cooperation and Development, 2016. Test No. 487. In: In Vitro Mammalian Cell Micronucleus Test, OECD Guidelines for the Testing of Chemicals, Section 4. OECD Publishing, Paris. https://doi.org/10.1787/9789264264861-en.

Palackal, N.T., Lee, S.H., Harvey, R.G., Blair, I.A., Penning, T.M., 2002. Activation of polycyclic aromatic hydrocarbon trans-dihydrodiol proximate carcinogens by human aldo-keto reductase (AKR1C) enzymes and their functional overexpression in human lung carcinoma (A549) cells. J. Biol. Chem. 277 (27), 24799–24808. https://doi.org/10.1074/jbc.M112424200.

Peixoto, M.S., da Silva Junior, F.C., de Oliveira Galvão, M.F., Roubicek, D.A., de Oliveira, Alves N., de Medeiros, S.R.B., 2019. Oxidative stress, mutagenic effects, and cell death induced by retene. Chemosphere 231, 518–527. https://doi.org/10.1016/j.chemosphere.2019.05.123.

Penning, T.M., 2017. Genotoxicity of ortho-quinones: reactive oxygen species versus covalent modification. Toxicol Res. 6, 740. https://doi.org/10.1039/c7tx00223h.

Ramdahl, T., 1983. Retene - a molecular marker of wood combustion in ambient air. Nature 306, 580–582. https://doi.org/10.1038/306580a0.

Rigaud, C., Eriksson, A., Krasnov, A., Wincent, E., Pakkanen, H., Lehtivuori, H., Ihalainen, J., Vehniainen, E.R., 2020. Retene, pyrene and phenanthrene cause distinct molecular-level changes in the cardiac tissue of rainbow trout (Oncorhynchus mykiss) larvae, part 1 - transcriptomics. Sci. Total Environ. 745, 141031 https://doi.org/10.1016/j.scitotenv.2020.141031.

Samburova, V., Zielinska, B., Khlystov, A., 2017. Do 16 polycyclic aromatic hydrocarbons represent PAH air toxicity? Toxics 5 (3), 17. https://doi.org/10.3390/toxics5030017.

Sarma, S.N., Blais, J.M., Chan, H.M., 2017. Neurotoxicity of alkylated polycyclic aromatic compounds in human neuroblastoma cells. J. Toxicol. Environ. Health - a: Curr. Issues 80, 285–300. https://doi.org/10.1080/15287394.2017.1314840.

Saxena, N., Phatak, P., Chauhan, V., 2022. Differential toxicity of abrin in human cell lines of different organ origin. Toxicol. in Vitro 78, 105250. https://doi.org/10.1016/j.tiv.2021.105250.

Scott, J.A., Incardona, J.P., Pelkki, K., Shepardson, S., Hodson, P.V., 2011. AhR2-mediated, CYP1A-independent cardiovascular toxicity in zebrafish (Danio rerio) embryos exposed to retene. Aquat. Toxicol. 101 (1), 165–174. https://doi.org/10.1016/j.aquatox.2010.09.016.

Shang, Y., Zhang, L., Jiang, Y., Li, Y., Lu, P., 2014. Airborne quinones induce cytotoxicity and DNA damage in human lung epithelial A549 cells: the role of reactive oxygen species. Chemosphere 100, 42–49. https://doi.org/10.1016/j.chemosphere.2013.12.079.

Shi, Q., Haenen, G.R., Maas, L., Arlt, V.M., Spina, D., Riffo Vasquez, Y., Moonen, E., Veith, C., Van Schooten, F.J., Godschalk, R.W.L., 2016. Inflammation-associated extracellular β-glucuronidase alters cellular responses to the chemical carcinogen benzo[*a*]pyrene. Arch. Toxicol. 90, 2261–2273. https://doi.org/10.1007/s00204-015-1593-7.

Shultz, C.A., Quinn, A.M., Park, J.H., Harvey, R.G., Bolton, J.L., Maser, E., Penning, T.M., 2011. Specificity of human aldo-keto reductases, NAD(P)H:quinone oxidoreductase, and carbonyl reductases to redox-cycle polycyclic aromatic hydrocarbon diones and 4-hydroxyequilenin-o-quinone. Chem. Res. Toxicol. 24, 2153–2166. https://doi.org/10.1021/tx200294c.

Tice, R.R., Agurell, E., Anderson, D., Burlinson, B., Hartmann, A., Kobayashi, H., Miyamae, Y., Rojas, E., Ryu, J.-C., Sasaki, Y.F., 2000. Single cell gel/comet assay: guidelines for in vitro and in vivo genetic toxicology testing. Environ. Mol. Mutagen. 35, 206–221. https://doi.org/10.1002/(SICI)1098-2280(2000)35:3<206::AID-EM8>3.0.CO;2-J.

Turner, M.C., Andersen, Z.J., Baccarelli, A., Diver, W.R., Gapstur, S.M., Pope, C.A., Prada, D., Samet, J., Thurston, G., Cohen, A., 2020. Outdoor air pollution and cancer: An overview of the current evidence and public health recommendations. CA Cancer J. Clin. 70, 460–479. https://doi.org/10.3322/caac.21632.

Urban, R.C., Alves, C.A., Allen, A.G., Cardoso, A.A., Campos, M.L.A.M., 2016. Organic aerosols in a Brazilian agro-industrial area: speciation and impact of biomass burning. Atmos. Res. 169, 271–279. https://doi.org/10.1016/j.atmosres.2015.10.008.

US EPA, 2011. Exposure Factors Handbook 2011 Edition (Final Report). U.S. Environmental Protection Agency, Washington, DC. EPA/600/R-09/052F. https://cfpub.epa.gov/ncea/risk/recordisplay.cfm?deid=236252 (Accessed 07 Dec 2022).

Vallabani, N.V.S., Alijagic, A., Persson, A., Odnevall, I., Sarndahl, E., Karlsson, H.L., 2022. Toxicity evaluation of particles formed during 3D-printing: cytotoxic, genotoxic, and inflammatory response in lung and macrophage models. Toxicology 467, 153100. https://doi.org/10.1016/j.tox.2022.153100.

Vicente, A., Alves, C.A., Monteiro, C., Nunes, T., Mirante, F., Cerqueira, M., Calvo, A., Pio, C., 2012. Organic speciation of aerosols from wildfires in Central Portugal during summer 2009. Atmos. Environ. 57, 186–196. https://doi.org/10.1016/j.atmosenv.2012.04.030.

Vicente, A., Calvo, A., Fernandes, A.P., Nunes, T., Monteiro, C., Pio, C., Alves, C.A., 2017. Hydrocarbons in particulate samples from wildfire events in Central Portugal in summer 2010. J. Environ. Sci. (China) 53, 122–131. https://doi.org/10.1016/j.jes.2016.02.022.

Wilsson, L.B., McClure, R.S., Waters, K.M., Simonich, M.T., Tanguay, R.L., 2022. Concentration-response gene expression analysis in zebrafish reveals phenotypically-anchored transcriptional responses to retene. Front Toxicol. 4, 950503 https://doi.org/10.3389/ftox.2022.950503.

Yu, Y., Katsoyiannis, A., Bohlin-Nizzetto, P., Brorstrom-Lunden, E., Ma, J., Zhao, Y., Wu, Z., Tych, W., Mindham, D., Sverko, E., Barresi, E., Dryfhout-Clark, H., Fellin, P., Hung, H., 2019. Polycyclic aromatic hydrocarbons not declining in Arctic air despite global emission reduction. Environ. Sci. Technol. 53 (5), 2375–2382. https://doi.org/10.1021/acs.est.8b05353.

Zhang, H., Zhang, X., Wang, Y., Bai, P., Hayakawa, K., Zhang, L., Tang, N., 2022. Characteristics and influencing factors of polycyclic aromatic hydrocarbons emitted from open burning and stove burning of biomass: a brief review. Int. J. Environ. Res. Public Health 19 (7), 3944. https://doi.org/10.3390/ijerph19073944.